ENGLISH VERSION

Analysis of the reinforcement of a steel structure with concentric diagonals. manta uvc case

Análisis del reforzamiento de una estructura de acero con diagonales concéntricas. caso del uvc de manta

Julia Pilatasig [*1], Roberto Aguiar [*,**] https://orcid.org/0000-0002-2771-1721, Brian Cagua [*] https://orcid.org/0000-0003-2530-8549, Oscar Andachi [*], Pablo Cerón [*] https://orcid.org/0000-0002-9519-7138

[*] Universidad de las Fuerzas Armadas ESPE, Quito, ECUADOR
[**] Universidad Laica Eloy Alfaro de Manabí, Manta, ECUADOR

Fecha de Recepción: 12/05/2021
Fecha de Aceptación: 29/09/2021
PAG 294-310

Abstract

The 2016 Pedernales earthquake affected several structures; one of them is the UVC of the city of Manta, in which a post-earthquake reinforcement with inverted-V diagonals was performed. This paper analyses the structure without reinforcement and with longitudinal reinforcement, using functions of the CEINCI-LAB Software to calculate displacements, drifts and floor shear in a seismic analysis using the spectral and static equivalent modal method with the 2016 Manta spectrum. In addition, the demand is established according to NEC-15 load combinations; live, dead and seismic load types. The earthquake effect is used for the verification of the axial capacity of the columns, considering the overstrength. After that, a design by capacity is carried out in the structure without reinforcement, based on the capacity of the beams, and in the case with reinforcement, an analysis based on the capacity of the diagonals is carried out. It is possible to observe that both the original structure and the reinforcement do not comply with the seismic design philosophy, and it is likely that an earthquake will cause damage in the future.

Keywords: Design by capacity; Structural reinforcement; Concentric bracing; CEINCI-LAB

Resumen

El sismo de Pedernales en 2016 causó afecciones a varias estructuras, un ejemplo es la UVC de la ciudad de Manta, en la cual se realizó un reforzamiento posterior al sismo, con diagonales en invertida. En este artículo se presenta un análisis de la estructura sin reforzamiento y con reforzamiento en sentido longitudinal, empleando funciones del Sistema Computacional CEINCILAB para determinar desplazamientos, derivas y cortante de piso, en un análisis sísmico con el método modal espectral y estático equivalente utilizando el espectro de Manta 2016. Además, se determina la demanda en función de las combinaciones de carga de la NEC-15, empleando los estados de carga viva, muerta y por sismo; para la comprobación de la capacidad axial de columnas se utiliza el efecto del sismo, considerando la sobre resistencia. Seguido de ello, se realiza un diseño por capacidad en la estructura sin reforzamiento, en función de la capacidad de las vigas y para el caso del reforzamiento se realiza un análisis en base a la capacidad de las diagonales. Se observa que tanto la estructura original como el reforzamiento no cumplen con la filosofía sismo resistente y es probable que se tenga afectación en un sismo en el futuro.

Palabras clave: Diseño por capacidad; reforzamiento estructural; arriostramientos concéntricos; CEINCI-LAB

1. Introduction

During the earthquake of Pedernales, Ecuador, on April 16, 2016 (Mw=7.8), the city structures were exposed to a real test on a natural scale. Now, it is important to analyze the design of damaged structures and how they were reinforced, with the aim of learning positive lessons to prevent these design errors in the future.

First, this paper analyzes the design of a steel structural block of the Unidad de Vigilancia Comunitaria (UVC)[1] in the city of Manta, whose masonry suffered considerable damage, and then studies how this block was reinforced.

(Figure 1) shows two pictures of the Manta UVC building. The picture on the left shows a 4-floor structure with cantilevers on the floor plan, which evidences great damage in the masonry, especially on the first floor, due to the lack of confining members. The picture on the right shows that, under the cantilever steel beam, there is no tie-bar to confine the block masonry.

[1] ***Corresponding author:***
Universidad de las Fuerzas Armadas ESPE, Quito. ECUADOR
E-mail: jepilatasig3@espe.edu.ec

Figure 1. *The staff's residential building of the Manta UVC is a 4-floor steel structure, withcantilevers in the floor plan only, whose masonry was largely damaged.*
Source: (Aguiar et al., 2016)

(Figure 2) shows the floor plan of the analyzed structure, which is 40.8 m long in the longitudinal direction and 13 m in the transverse direction, so that the length/width aspect ratio is 3:14. This ratio indicates that it is an elongated structure, which will probably have torsion problems on the floor plan. The structural behavior could be enhanced with a ratio of 2, which is feasible through a construction joint.

The configuration in the transverse direction shows two overhangs on the floor plan only, one of 2.65 m on one side and another of 1.15 on the opposite side. The existing masonry under the cantilevers have no confining members and were seriously damaged, as shown in (Figure 1). If confining members had been used, these damages could probably have been reduced.

(Figure 2) evidences that all columns are "I" type (HEA) and placed in the same direction. The transverse direction is the strongest, considering that the span to be covered is 9.2 m (rigid frames 1 to 5 and 8 have 2 column rows/axis). The columns act on the weakest section in the longitudinal direction. Their behavior could be improved by alternating the direction of the columns.

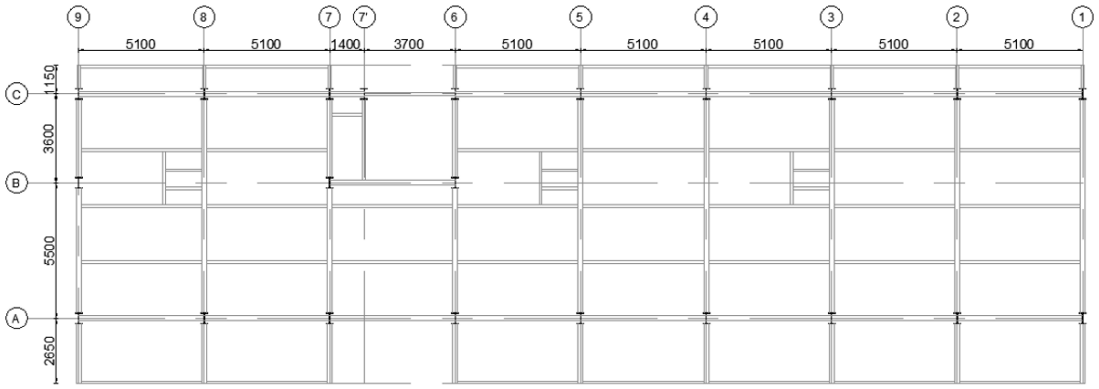

Figure 2. *Floor plan view with the direction of the columns and dimensions of the openings.*

[1] *Citizen security service depending from the State Police and the Prosecutor's Office.*

A positive feature of this structure is that it was built with bolted flange plate (BFP) connections, which acted on the elastic range during the 2016 earthquake. Therefore, these connections are considered to have a good behavior. It is not known if it was confirmed that the bolt torque of the structural reinforcement was greater than 220 ft-lb., which is advisable for this connection. The left side of (Figure 3) shows a BFP connection and the right side, the cross sections of columns (height of 430 mm) and beams (height of 500 mm).

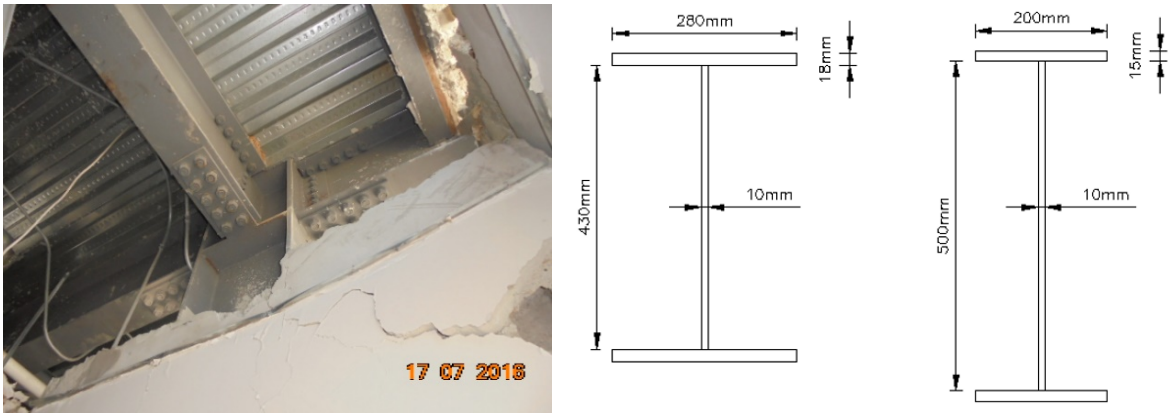

Figure 3. *BFP connection and profiles used in columns and beams. Source: (Aguiar et al., 2016)*

2. Structural analysis during the 2016 earthquake

Rigid frame A, whose columns act on the weak direction, is analyzed with an educational purpose and because it allows obtaining the highest possible number of results. This rigid frame is assessed considering the spectrum of the EW component, which was found on the record obtained in the Manta 2016 earthquake (Mw=7.8), hereafter called the Manta Spectrum. The seismic analysis uses the Spectral Method (based on the modal combination criterion of Complete Quadratic Combination, CQC) and the Static Method according to the Ecuadorian Building Standard NEC-15, but working with the Manta Spectrum.

The procedure carried out with the CEINCI-LAB software will be indicated as the results are obtained. The theoretical framework and how the software was used is detailed in (Cagua et al., 2021) and (Andachi and Cerón, 2021).

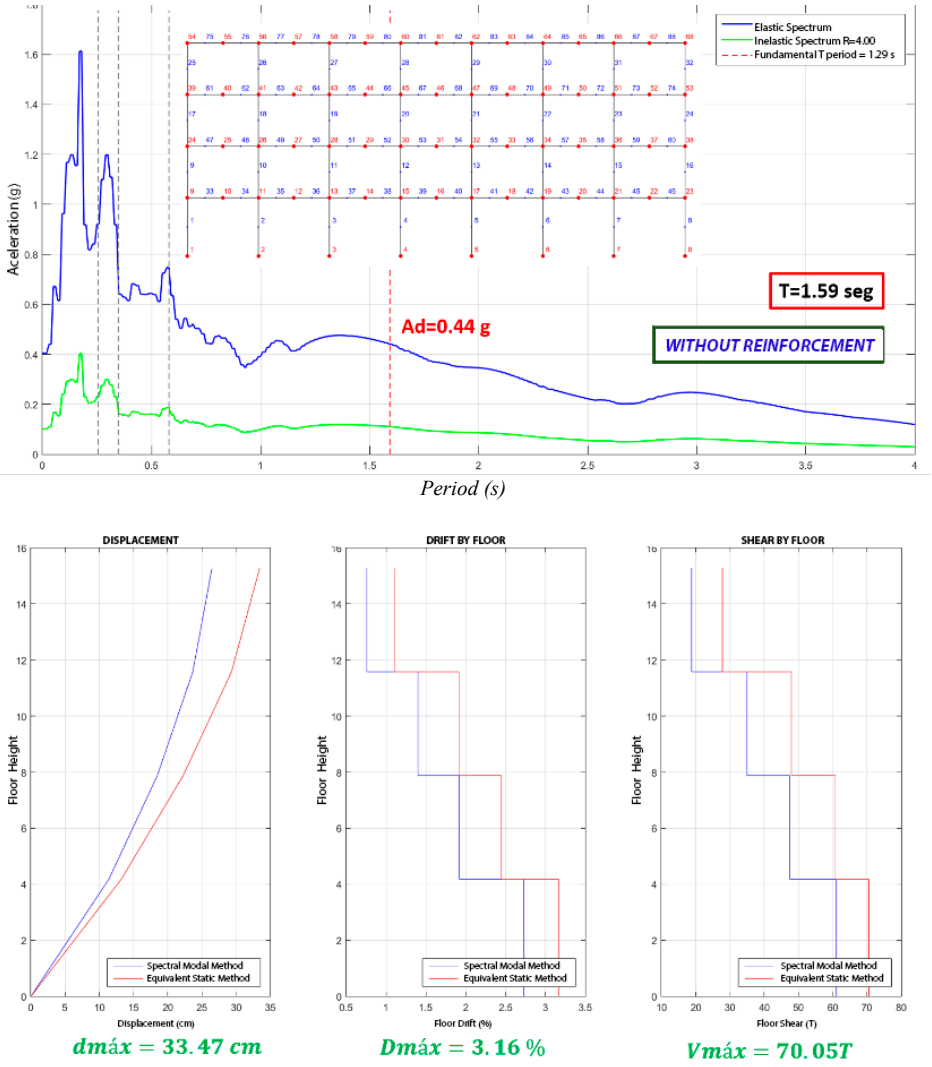

Figure 4. *The upper chart presents the elastic and inelastic spectra for R=4; the bottom chart shows the maximum responses for displacements, floor drifts and floor shea*

The seismic analysis considers a seismic force reduction factor of R=4, because the structure does not have much redundancy in the longitudinal direction (2 column rows/axis). Usually, structural designers work with the highest R-value provided in seismic regulations, without verifying at the end of the analysis whether the designed structure is actually capable of having that R-value.

Furthermore, it is inconvenient to work with high R-values, since the spectrum is strongly reduced; see the indications in the above chart (Figure 4). When working with R-values that are too high, the design considers seismic forces that are too low and the structure enters the non-linear range, thus producing damages that owners will not accept (Aguiar, 2017). It is advisable to work with low R-values so that the members will have a high ductility.

The resulting fundamental T period of the structure is 1.59 s, which is a very high value for a 4-floor structure. This is a consequence of the direction of the columns acting on the weak side (for rigid frame A); consequently, it is advisable to place the "I" profile columns alternately.

The maximum floor drift resulting from the two analysis methods is higher than 2%. This value, which is higher than that allowed by design standards, leads to believe that the structure may have suffered some damage. The false ceiling makes it very hard to see the damage; however, when carefully observing all the nodes of the floor plan to see the behavior of BFP connections, no damage was evidenced.

The structure's stability index (θ) is calculated. This factor is related to the P-Delta effect, which allows assessing the structural stability in the face of a possible overturning, and it is calculated with (Equation 1). These additional effects may increase the internal forces, moments and drifts.

$$\boldsymbol{\theta_i = \frac{P_i \cdot \Delta_i}{V_i \cdot h_i}} \qquad \textbf{(1)}$$

In this expression, Pi is the axial load due to the dead and live load types; Δi is the relative elastic displacement of each floor; V_i is the shear in each level and h_i is the height of each level. When the stability index is below 0.10, the floors are classified as not liable to overturn. When this index is higher than 0.3, the structure is potentially unstable and should be stiffened. When values are between 0.1 and 0.3, a factor of $f_{p\text{-}\Delta}$ must be calculated and all lateral loads should be multiplied by this factor.(Equation 2).

$$\boldsymbol{f_{P-\Delta} = \frac{1}{1-\theta}} \qquad \textbf{(2)}$$

Where θ is the highest value of θ_i. The factor for each floor is indicated below. Floor 1 shows a factor slightly greater than 0.10, which implies that calculations must consider the P-Delta effect with factor $f_{p\text{-}\Delta}$.

$$\theta = \begin{bmatrix} 0.1182 \\ 0.0694 \\ 0.0459 \\ 0.0230 \end{bmatrix}$$

The table D1.1 of AISC 341-16 is used for calculating the compactness of each member, which classifies sections into highly ductile (HD), moderately ductile (MD) and non-ductile (ND). First, the aspect ratio for the flange b/t_f was obtained, where b is half the width of the flange and t_f is the flange thickness. In all cases, this ratio was lower than λ_{nd}, therefore, it is highly ductile. Then, the aspect ratio in the web h/t_w was obtained, where h is the web height and t_w, its thickness. In this case, the profiles were also highly ductile. (Figure 5) shows the results, showing that all members are highly ductile.

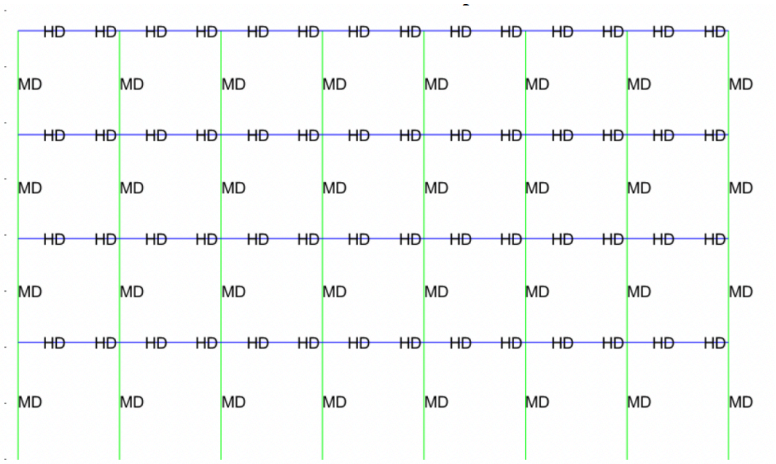

Figure 5. *Compactness of structural members using table D1.1 of AISC 341-16*

If the flange and the web are highly ductile, the analyzed section is highly ductile. If one of them is not, they pass to the next category, which is moderately ductile, and so on. Regarding the web, the calculation of λ_{nd} is a function of a factor C_a, which in turn depends on the acting axial load P_u.

Once the equivalent static forces for the Manta earthquake spectrum (Load Type E) were obtained, the rigid frame was statically determined four times, that is: (i) with just the dead load DL; (ii) with just the live load LL; (iii) with seismic forces from left to right (Ep); (iv) with seismic forces from right to left (E_N). These results allowed obtaining the following load combinations:

$$i)\ CM + CV\ M + CV \qquad ii)\ 1.4 \cdot CM \qquad iii)\ 1.2 \cdot CM + 1.6 \cdot CV$$
$$iv)\ 1.2 * CM + CV \qquad v)\ 1.2 \cdot CM + CV + \Omega \cdot E_P \qquad vi)\ 1.2 \cdot CM + CV + \Omega \cdot E_N$$
$$vii)\ 0.9 \cdot CM \qquad viii)\ 0.9 \cdot CM + E_P \qquad ix)\ 0.9 \cdot CM - E_N$$

The variable that has not yet been indicated is the overstrength Ω, which has a value of 3 for unbraced rigid frames and 2.5 for braced rigid frames (ASCE 7-16). This factor applies only in the event of axial loads in the columns. The maximum and minimum values for axial force, shear and moment (demand D) were obtained from the nine (9) load combinations. Moreover, the capacity C of the sections was obtained.

The axial capacity is assumed as the compressive capacity in relation to the weak axis of the section. This is the most critical condition, because the yield point is reduced based on the slenderness ratio of the members. Therefore, (Equation 3) is applied, where Ag is the area of the cross section. Moreover, (Equation 4) and (Equation 5) are used for calculating the critical stress and the Euler critical stress. The effective length method is applied, that is, K-factors are directly calculated for each member based on the boundary conditions (G-factors). In order to program this methodology, the French curve ruler is used, as indicated in (Equation 6).

$$P_n = F_{cr} * A_g \qquad \textbf{(3)}$$

$$Fcr_{EULER} < 0.44 \cdot F_y \rightarrow F_{cr} = 0.877 * Fcr_{EULER}$$
$$Fcr_{EULER} \geq 0.44 \cdot F_y \rightarrow F_{cr} = 0.658^{\frac{F_y}{Fcr_{EULER}}} * F_y \qquad \textbf{(4)}$$

$$Fcr_{EULER} = \frac{\pi^2 \cdot E_s}{\left(\frac{K \cdot L}{r}\right)^2} \qquad \textbf{(5)}$$

$$K = \sqrt{\frac{1.6 \cdot G_A \cdot G_B + 4 \cdot (G_A + G_B) + 7.5}{G_A + G_B + 7.5}} \qquad \textbf{(6)}$$

The shear capacity is calculated with (Equation 7), where A_w is the area resisting the shear (Equation 8) and Cv1 depends on the aspect ratio of the member's web (Equation 9).

$$Vn = 0.6 \cdot F_y \cdot A_w \cdot Cv_1 \qquad \textbf{(7)}$$

$$A_w = (d - 2 \cdot tf) \cdot tw \qquad \textbf{(8)}$$

- *When*

$$\frac{h}{tw} \leq 1.1 \cdot \sqrt{\frac{k_v \cdot E}{F_y}}$$
$$Cv_1 = 1$$

- *Or else*

$$Cv_1 = \frac{1.1 \cdot \sqrt{\frac{k_v \cdot E}{F_y}}}{h/t_w} \qquad \textbf{(9)}$$

The flexural capacity depends on the unbraced length of the members and the compactness of the latter. This case assumes that the members are able to develop their maximum plastification capacity, as shown in (Equation 10).

$$M_n = M_p = F_y \cdot Z_x \qquad \textbf{(10)}$$

Where Z_x is the plastic section modulus with regard to the flexural axis of the member. The effects of flexural and axial load are related; therefore, the flexural and axial strength of the members acting under these effects should be verified based on (Equation 11).

$$For \quad \frac{P_u}{\emptyset \cdot P_n} \geq 0.2 \quad \rightarrow \quad \frac{P_u}{\emptyset \cdot P_n} + \frac{8}{9} \cdot \frac{M_u}{\emptyset \cdot M_n} \leq 1$$

$$For \quad \frac{P_u}{\emptyset \cdot P_n} < 0.2 \quad \rightarrow \quad \frac{P_u}{2 \cdot \emptyset \cdot P_n} + \frac{M_u}{\emptyset \cdot M_n} \leq 1 \qquad \textbf{(11)}$$

Demand D and capacity C allow calculating the D/C ratio; each member has two values in the initial and final nodes. The values indicated in (Figure 6) and (Figure 7) are the most critical.

.

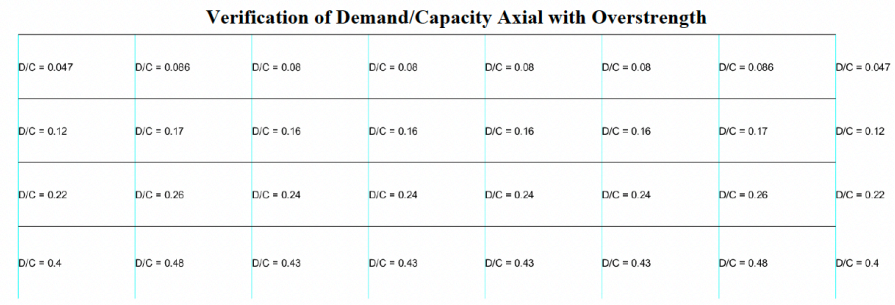

Figure 6. Column D/C ratio for axial load, considering overstrength

(Figure 6) shows the D/C compression ratio in columns, and demonstrates that all values are lower than one, which is correct. Now, the upper table of (Figure 7) indicates the ratio to bending in the beams and flexural compression in the columns. Here, the beams present no problems, however, the columns do, especially the columns on the first floor, whose D/C ratio is greater than one. Now, it should be highlighted that all columns were coated with concrete, thereby forming mixed sections, which contributed to improve the column capacity, thus preventing post-earthquake damages in these members (Aguiar et al., 2016a).

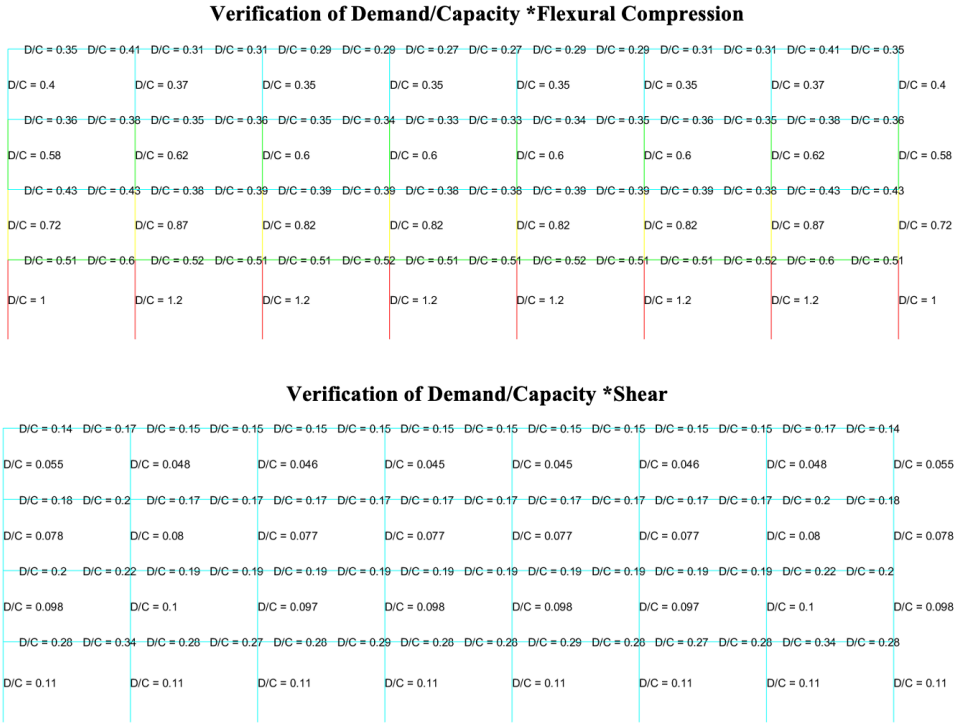

Figure 7. *Upper table: D/C ratio to flexural compression in columns and bending in beams; bottom table: D/C ratio to shear*

The D/C ratio to shear is indicated at the bottom of (Figure 7); the values are lower than one, which is fine. (Figure 8) shows the ratio of the summation of beam moments reaching a node of $\Sigma M\dot{p}v$, to the summation of column moments $\Sigma M\dot{p}\ c$. This ratio is hopefully lower than one, so that the column is stronger than the beam, which is represented in (Equation 12). In the analyzed structure, all nodes have a ratio greater than one, which means that the beams are stronger than the columns and, therefore, the design is not aligned with the earthquake-resistant philosophy.

$$\frac{\sum M\dot{p}v}{\sum M\dot{p}c} \leq 1.0 \qquad \textbf{(12)}$$

Verification of Capacity *Beam/Column

Vg/Col = 3.9	Vg/Col = 8	Vg/Col = 8	Vg/Col = 8	Vg/Col = 8	Vg/Col = 8	Vg/Col = 8	Vg/Col = 3.9
Vg/Col = 2	Vg/Col = 4.1	Vg/Col = 4.1	Vg/Col = 4.1	Vg/Col = 4.1	Vg/Col = 4.1	Vg/Col = 4.1	Vg/Col = 2
Vg/Col = 2.1	Vg/Col = 4.4	Vg/Col = 4.4	Vg/Col = 4.4	Vg/Col = 4.4	Vg/Col = 4.4	Vg/Col = 4.4	Vg/Col = 2.1
Vg/Col = 2.4	Vg/Col = 5.1	Vg/Col = 5	Vg/Col = 5	Vg/Col = 5	Vg/Col = 5	Vg/Col = 5.1	Vg/Col = 2.4

Figure 8. *Moment capacity ratio in beams to columns at the nodes*

3. Structural reinforcement

In order to proceed with the reinforcement, all the walls were demolished, regardless of the fact that the damage was concentrated on the first floor. Afterwards, the concrete within the "I" Columns was eliminated. Last, all subfloors were removed because of their great thickness. The demolishing process was carried out with a sledgehammer manipulated by one person. In this respect, it is unknown whether the steel of the columns or the concrete placed on top of the steel deck were damaged after this work was completed. The purpose of the work was to reduce the weight, which is a positive aspect, so that when the reinforcement is done, the total weight of the structure will be equal or slightly higher than the structure without reinforcement. However, the constructor must make sure that the methods used will not affect the structure during the process.

The structure was reinforced with inverted-V steel bracing systems in the openings indicated in (Figure 9a); four openings in the longitudinal direction and two openings in the transverse direction (blue line), and in all floors of the structure, as shown in (Figure 9b). It should be noted that, on the second floor, a block wall is built in the back of the diagonals. (Figure 9c) shows the reinforcement in the floor plan, and it is possible to see that all the false ceilings have been removed, as well as the concrete within the "I" type columns. It is worth mentioning that no reinforcement at all was made in the foundation (Aguiar et al., 2017). Finally, (Figure 9d) shows that the upper Gusset plate for the diagonals is not fastened; the latter were rather welded directly to the beams. This is not advisable, because if one diagonal enters the non-linear range and the decision is made to change this member after the earthquake, it is likely that it will somehow affect the beam in this direction. The recommendation is to use bolted and welded connections to join diagonals to the upper Gusset plate.

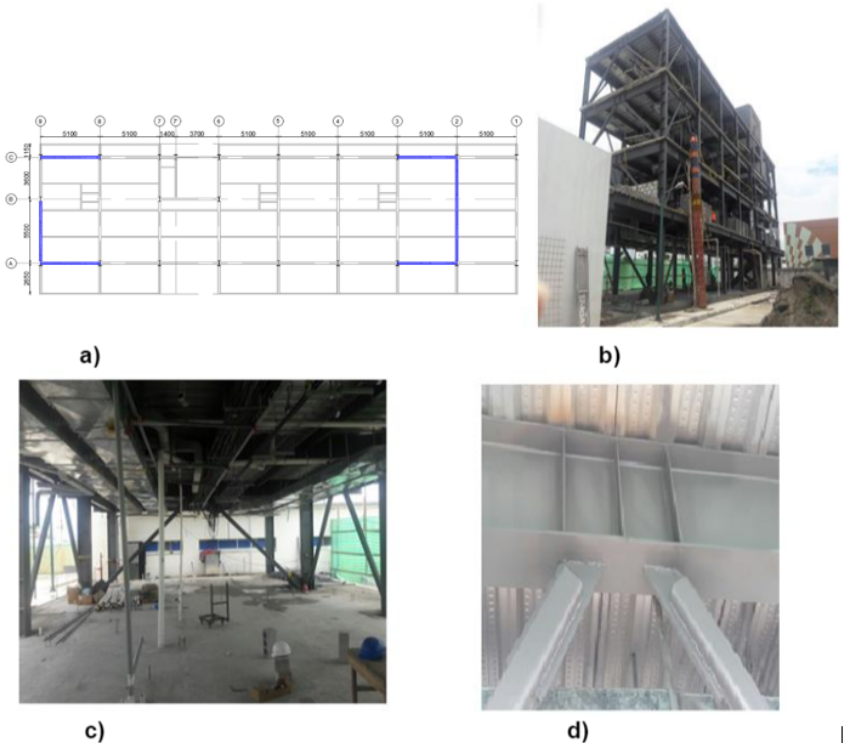

Figure 9. *Seismic reinforcement of the Manta UVC; a) Floor plan view and location of reinforced openings; b) Panoramic view of the structure reinforced with inverted-V concentric diagonals; c) Floor plan view showing the columns without concrete and their direction; d) Stiffeners in the beam and diagonals. Source: (Aguiar et al., 2017)*

(Figure 10) shows the reinforcement of rigid frame A, where concentric bracing is placed in the openings in both ends. This figure allows observing that the diagonals are classified as highly ductile sections. It should be mentioned that the sections are 150 mm square tubes with thickness of 15 mm, as evidenced in (Figure 9d).

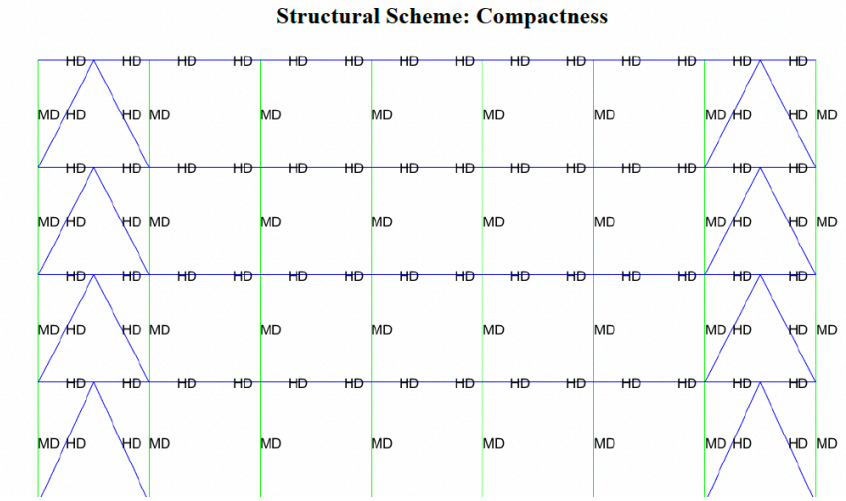

Figure 10. *Compactness of structural members using table D1.1 of AISC 341-16*

The structure is stiffened when bracing elements are included and the period decreases to 0.40s, corresponding to a 75% reduction. The spectral acceleration in the fundamental vibration mode increases to 0.62 g, and the displacements, drifts and shear in each floor can be appreciated in (Figure 11). In this case, a positive aspect is that the maximum drift decreases to 0.34%, which is much lower than the 2% limit specified in NEC-15.

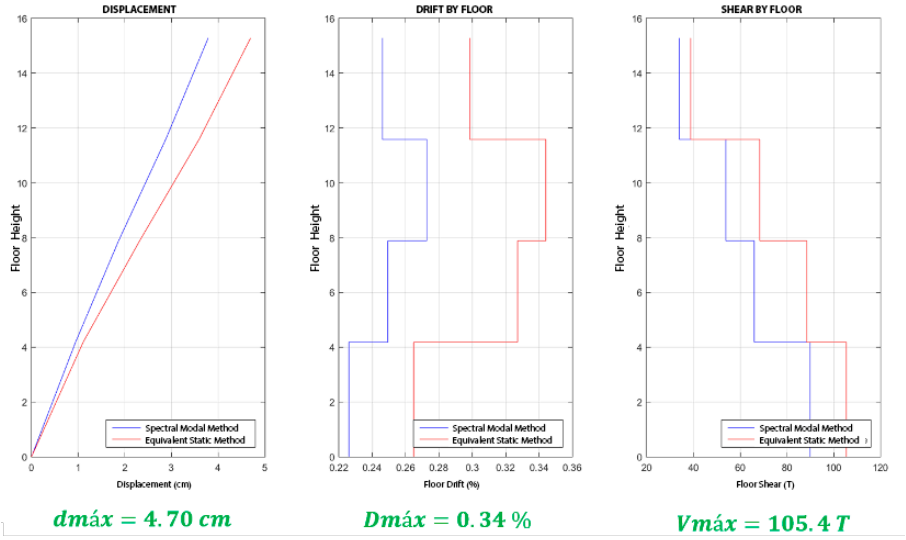

Figure 11. *Maximum responses for displacements, floor drifts and floor shear*

(Figure 12a) presents a chart of the axial D/C ratio, considering the effect of overstrength for the columns. It evidences that the demand decreases and, therefore, the D/C ratio is compliant in this case. (Figure 12b) shows the results for the flexural compressive strength in columns, bending strength in beams and axial load in diagonals; likewise, (Figure 12c) shows the D/C ratio to shear.

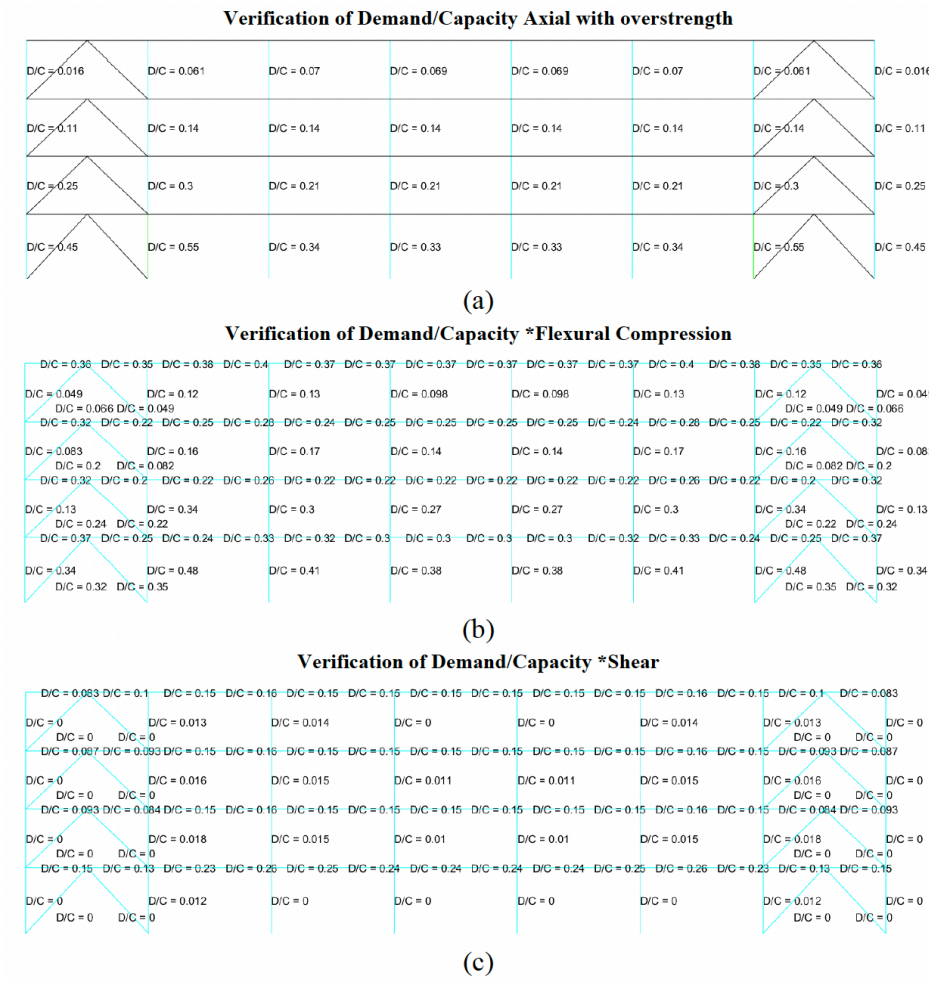

Figure 12. *D/C ratio for: a) axial load in columns considering overstrength; b) flexural compression in columns, bending in beams and axial load in diagonals; c) shear strength*

When analyzing the weak-beam-strong-column relationship (Equation 12), it is possible to see that the values are still greater than one, that is, during an earthquake the columns could fail before the beams do, and that is not convenient for the seismic performance of the structure.

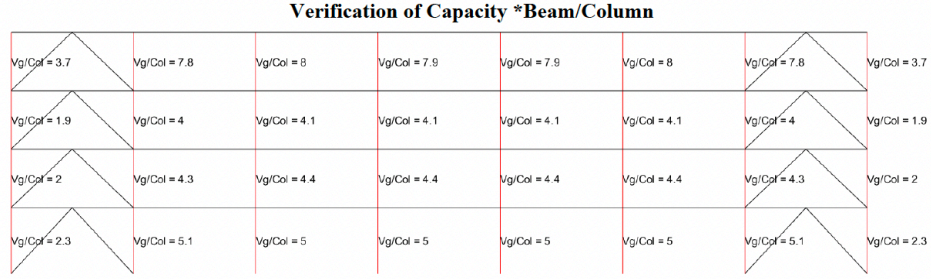

Figure 13. *Moment capacity ratio in beams to columns at the nodes*

In rigid frames with systems resisting lateral loading based on columns and beams together with diagonals, that is, dual rigid frames, it is important to know the shear value that diagonals withstand and the percentage that columns withstand. In this case, it is possible to observe that the diagonals resist more than 90% of the earthquake in the first 3 floors, and 87% in the fourth floor (Figure 13). Although this can be positive, the columns should comply with resisting at least 25% of the seismic force, because if the diagonals should fail, the columns should be able to secure the lateral loading system. This requirement is fulfilled, since it was previously demonstrated that the Columns were resisting 70 T (Figure 14), which is approximately 70% of 105.4 T (Figure 11). Moreover, it confirms that the main rigid frame has the capacity to resist gravitational loads without the support of diagonals in the beams.

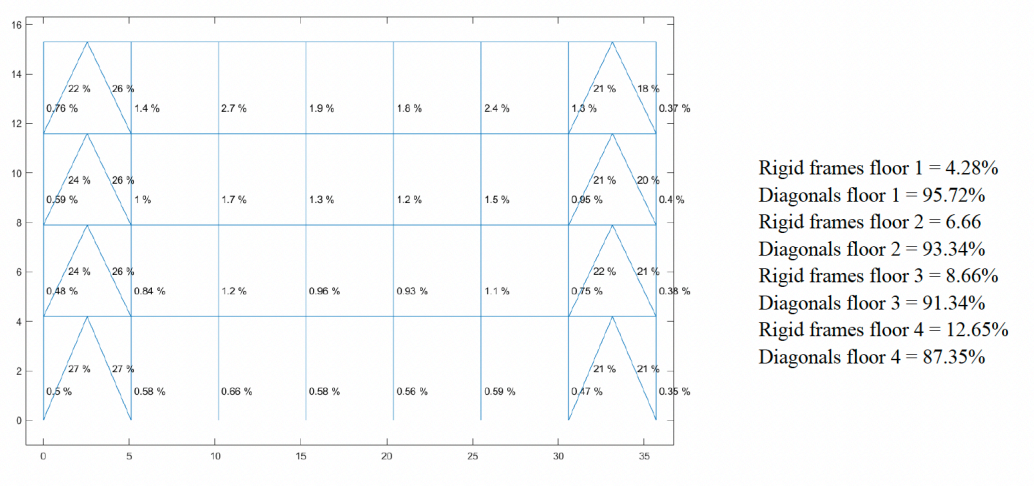

Figure 14. *Seismic forcé percentage that Columns and diagonals resist in the event of an earthquake from left to right*

4. Control of the forces at the joint of the diagonals

Up to this point, the analysis with reinforcement seems positive, since the forces in the beams and columns are redistributed to the diagonals, thus generating D/C values below those in the original case. Additionally, the stability indexes decrease to values much lower than 0.1, which means that the reinforced structure is not liable to overturn. Nevertheless, in order to complete the analysis, a capacity design should be carried out, according to Chapter F of the seismic provisions in AISC 341-16. For rigid frames with special bracing, it is specified that the seismic demand in columns, beams and connections should be obtained from the capacity expected from the diagonal, whose effect must be calculated as the highest from the following analyses:

a) An analysis assuming that all bracing resist forces corresponding to their expected compressive or tensile strength.

b) An analysis assuming that all bracing under tensile stress resist forces corresponding to their expected strength, and it is assumed that all bracing under compressive stress resist forces based on their expected compressive strength post buckling.

The resistance expected from the bracing system under tensile stress can be obtained with (Equation 13). Furthermore, the resistance expected from the bracing system under compressive stress must be the lowest one among the values resulting from (Equation 13) and (Equation 14). The calculation of the bracing resistance expected after buckling should consider a maximum of 0.3 times the bracing resistance expected in compression.

$$F_T = R_y \cdot F_y \cdot A_g \qquad \textbf{(13)}$$

$$F_c = \frac{1}{0.877} \cdot F_{cr} \cdot A_g$$

$$F_c = 0.3 \left(\frac{1}{0.877} . F_{cr} \cdot A_g \right)$$

$$F_c = 0.34 . F_{cr} \cdot A_g \qquad \textbf{(14)}$$

In order to calculate F_{cr}, R_y F_y should be used instead of F_y in (Equation 4).

The above is called Case a and Case b of the capacity design in rigid frames with concentric bracing, which is graphically explained in (Figure 15a) and (Figure 15b), where CE is the compression expected and TE is the tension expected from the braces.

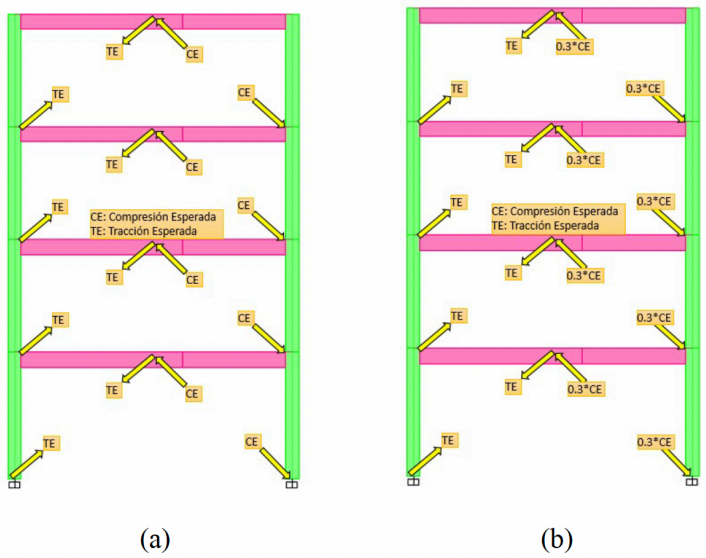

Figure 15. *a) Application of maximum expected forces given the capacity of the diagonals (Case a); b) application of expected tension and compression forces post buckling (Case b).*

Since the expected tension and compression forces have different numerical values, there could be unbalanced forces at the node. This implies a horizontal and a vertical component acting on the beam, which will produce internal axial, shear and bending actions at the beam and the column. The vertical force resulting from unbalanced forces is called Pun, as shown in (Figure 16).

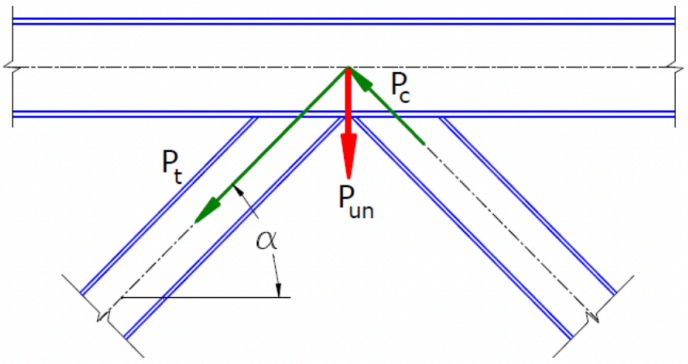

Figure 16. *Pun force resulting from unbalanced forces at the node, due to tensile and compressive forces. Source: (Crisafulli, 2014)*

The structure is stiffened when bracing elements are included and the period decreases to 0.40s, corresponding to a 75% reduction. The spectral acceleration in the fundamental vibration mode increases to 0.62 g, and the displacements, drifts and shear in each floor can be appreciated in (Figure 11). In this case, a positive aspect is that the maximum drift decreases to 0.34%, which is much lower than the 2% limit specified in NEC-15.

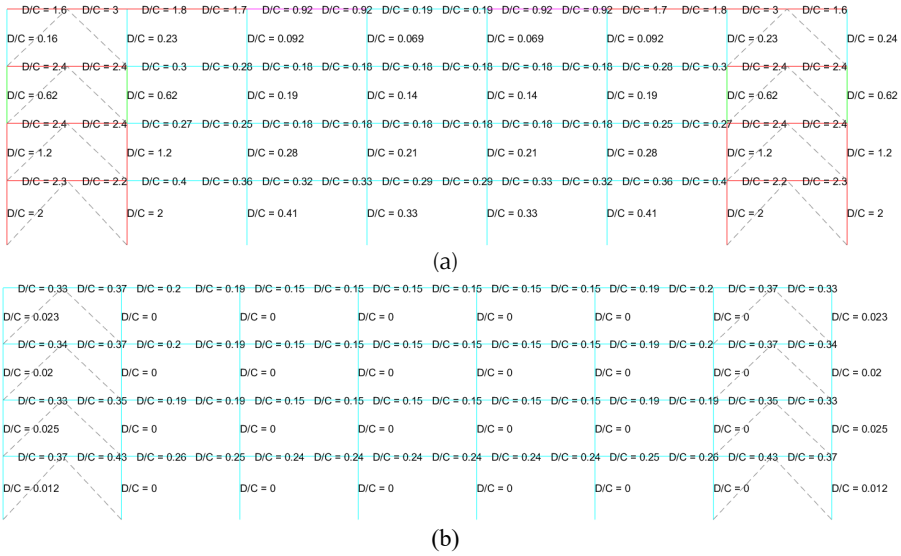

Figure 17. *D/C ratio for: a) axial load in columns considering overstrength; b) axial loads in columns and flexural-axial loads in beams; c) shear strength*

Case b *of the analysis, with regard to the capacity of the diagonals, shows a similar scenario (Figure 15b). This case considers the expected post-buckling compressive strength and there is a greater unbalance of forces in the beams' midpoint node (joint of the diagonals). This implies greater loads and, consequently, the philosophy of maintaining the rigid frame of columns and beams within the elastic range during an earthquake is likely to fail, as observed in (Figure 18). In this case, the shear demand on beams to which the diagonals are connected to increases to almost 60% due to these unbalanced forces (Pun force).*

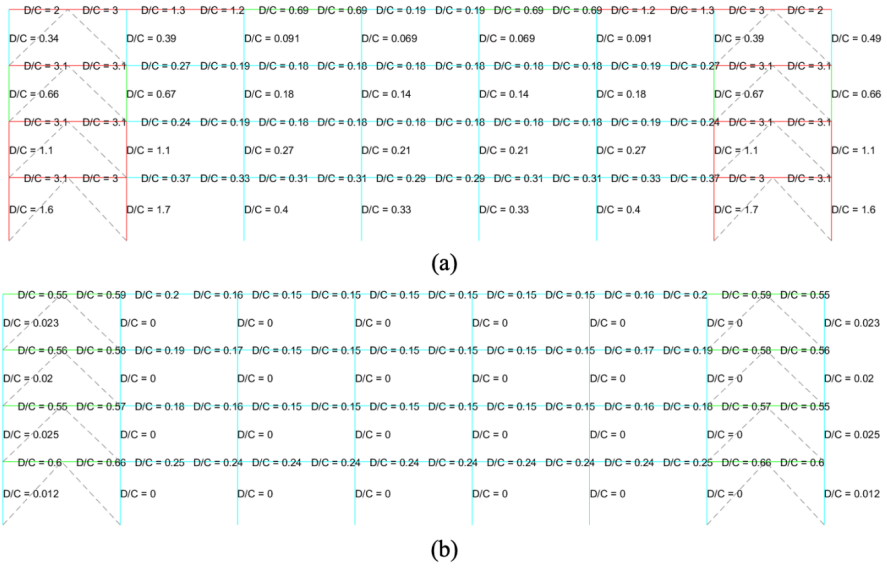

Figure 18. *D/C ratio for: a) axial load in columns considering the overstrength, b) axial loads in columns and flexural-axial loads in beams; c) shear strength*

5. Applicability in other structures

The functions developed in the CEINCI-LAB computer system are presented in an interface enabling the user to analyze different types of structures. The analysis presented in this document can be applied to any type of steel structure without reinforcement and with inverted-V bracing system. The functions used allow knowing the displacements, drifts, and floor shears of a structure exposed to seismic loads, similar to those of the earthquake of April 16, 2016 in Pedernales, Ecuador. In addition to the D/C ratio, which is a parameter that defines whether the structure complies or not, with resistance parameters of the earthquake-resistant design philosophy. The use and theoretical support of these functions are detailed in (Cagua et al., 2021) and (Andachi and Cerón, 2021), which evidence that the functions have been developed for structures with different geometries.

One of the parameters used for the seismic analysis is the reduction factor of the seismic forces R, which varies according to the structuring and is detailed in the standards. For this particular case, its value is R=4, because the structure has not much redundancy in the longitudinal direction (2 column rows/axis) and, moreover, the existing structure has suffered the action of several earthquakes.

The application of this type of analysis will allow knowing the characteristics and behavior of a structure exposed to seismic loadings and its results will enable to take preventive measures to avoid damages in an existing structure and improve the features of future designs.

6. General recommendations

The design of any type of structure is governed by legal regulations, which specify the design features that must be strictly complied with. However, the following paragraphs provide general recommendations regarding the design of steel structures without reinforcement and reinforced with inverted-V diagonals.

Works such as that of (Aguiar et al., 2017) have evidenced the damage levels in the masonry, particularly in the structures affected by the 2016 earthquake in Pedernales. Therefore, the recommendation is to include confining members in the masonries, with the aim of preventing or reducing the damages.

Within the structural configuration of the floor plan, a length/width ratio of 2 or less should be maintained to avoid the torsion in the floor plan.

The location of all the columns, with I-type sections and in the same direction, causes one of the analyzed directions to have the weakest section, which entails an inadequate behavior of the floor plan. This behavior can be improved by alternating the direction of the columns.

Although the seismic reduction factor R is governed by legal regulations, according to the type of structural configuration, it is not advisable to use high R-values, because it reduces the spectrum and, consequently, decreases the designed seismic forces, which causes the structure to enter a non-linear range and to suffer damages.

The fact of including bracing systems in a rigid frame stiffens the structure and reduces its period, as well as the drifts and displacements, which improves the behavior of the structure. However, this inclusion should take into account that the demand of these braced rigid frame members (beams and columns) should not exceed their capacity, in order to preserve the earthquake-resistant design philosophy, by checking up that all structures follow the principle of weak diagonal-strong beamstronger column. Here, it is important to mention that commercial structural design software do not automatically include all load types in the analysis, which means that the designer should envisage particular cases in their analyses. The CEINCI-LAB software has programmed these specific cases, therefore, designing with the functions developed by CEINCI-LAB offers an advantage for the analysis and design of this type of structures.

It is important to calculate the unbalanced forces generated at the joint of the beam and the diagonal, and to remember the relevance of correctly designing this member to prevent damages in non-desired places, thus complying with the philosophy of energy dissipation through the diagonals.

After the 2016 earthquake in the Province of Manabí, several structures were damaged at different levels, and some of them were modified when the need to implement a reinforcement to keep its usefulness was evidenced. The work of (Aguiar et al., 2016) details the importance of reinforcing structures subjected to the effects of an earthquake, thereby mentioning damages in four specific cases, located in the province of Manabí. On the other hand, works such as those by (Lara et al., 2018) present the main failure causes of RC framed structures. The use of bracing diagonals is one of the most common methods for reinforcing rigid frames. However, specifically in Manabí, the structures were modified according to their requirements; the detail of these works was presented in (Aguiar, 2017).

Chapter 5 of the book of (Aguiar et al., 2017) describes the reinforcement of the Manta UVC, the structure studied in the present paper. However, the reinforcement mechanism includes energy dissipators. The analyses allow

suggesting that when the beam above the concentric diagonals does not have enough flexural and shear strength, it is best to place energy dissipators above the diagonals.

7. Observations and conclusions

The direction of the columns in the floor plan generates a weak direction of the structure in the longitudinal direction; in this case, it is liable to torsion in the floor plan. Moreover, there is low lateral stiffness reflected by a high vibration period, which entails large displacements, with drifts around 3.16% that allow anticipating great damage after an earthquake.

The linear static analysis does not allow visualizing the appearance and sequence of the damage produced in the members. Nevertheless, in a conservative way, this analysis allows evidencing the demand/capacity ratio of the members in the face of different load demands. In this case, it is evident that the structure has problems and does not comply with the weak beam-strong column design philosophy. It neither presents a behavior of weak diagonal-strong beam-stronger column, which is adequate for the energy dissipation based on the damage without compromising the lateral stability and global integrity of the structure.

The reinforcement seems to improve the behavior of the structure in terms of improving the stiffness, reducing displacements and drifts, and reducing the demand on columns and beams under different loading conditions. However, the capacity design reveals that it is not advisable to place steel diagonals without reinforcing beams and columns. Further analyses are recommended, as well as taking corrective measures in a timely manner before a new earthquake occurs in Ecuador.

Using the functions of the CEINCI-LAB software helps making a step-by-step analysis, where the user can clearly appreciate the calculations through the matrix analysis.

A structural reinforcement with concentric diagonals is a valid option; however, all the members forming the new reinforced frame should be carefully analyzed, with the aim of guaranteeing an earthquake-resistant design.

8. References

Aguiar, R. (2008). Análisis Sísmico de Edificios. Quito : Centro de Investigaciones Científicas. Escuela Politécnica del Ejército.

Aguiar, R. (2017). No se acepta el diseño por ductilidad. Caso del Edificio Fragata que incursionó en el rango no lineal. Revista Internacional de Ingeniería de Estructuras, 22(3): 327-391.

Aguiar, R.; Del Castillo, F.; Ávila, V.; Coyago, H.; Cedeño A. (2017). Diseño de contraviento y placa Gusset de conexión para soportar disipadores de energía. Revista Internacional de Ingeniería de Estructuras, 22 (2), 227-249. doi: http://www.riie.espe.edu.ec.

Aguiar, R.; Zevallos, M.; Palacios, J.; García, L.; Menéndez, E. (2016a). Reforzamiento de estructuras con disipadores de energía. Terremoto de Ecuador del 16 de abril de 2016. Quito: Instituto Panamericano de Geografía e Historia IPGH, Primera Edición. p. 287.

Aguiar, R.; Zevallos, M.; Palacios, J.; García, L.; Menéndez,. E. (2016). Necesidad de Reforzar las Estructuras afectadas por un Terremoto. Revista de Investigaciones de Energía Medio Ambiente y Tecnología REIMAT, 1(1), 17-24.

Aguiar, R.; Andrango, K.; Araujo, A.; Aroca, J.; Arostegui, M.; Burbano, A.; Bustamante, L.; Cando, D.; Cevallos, A.; Chamorro, M.; Chipantiza, K.; Criollo, D.; Erazo, J.; Estacio, S.; Gaibor, K.; Guacho, J.; Hidalgo, J.; Luje, D.; Nacevilla, L.; Rueda, J. (2017). Structural Behavior of Buildings Affected By the 2016 Earthquake in Manta. First Part. Revista Ciencia, 19(3), 363–387.

Aguiar R. (2017). Reforzamiento de estructuras afectadas por el terremoto del 16 A. Primera parte. Conferencia por los 89 de creación del Instituto Panamericano de Geografía e Historia IPGH. Quito, Ecuador.

Aguiar, R.; Cagua, B.; Pilatasig, J. (2021). Calculation of the Dynamic Properties of a Structure with CEINCI-LAB and Application to the Reinforcement of the ULEAM Parking Building. Revista Internacional de Ingeniería de Estructuras, 26 (2), 364-425.

Andachi, O.; Cerón, P. (2021). Disposiciones especiales para el diseño de estructuras de acero con diagonales concéntricas. Quito: Universidad de las Fuerzas Armadas ESPE.

AISC/ANSI (2016). AISC/ANSI 360-16 Specification for Strcutural Steel Building. American Institute of Steel Construction (AISC).

AISC/ANSI. (2016). ANSI/AISC 341-16 Seismic Provisons for Strutural Steel. American Institute of Steel Construction (AISC).

ASCE/SEI 7-16. (2016). Minimum Design Loads and Associated Criteria for Buildings and Other Structures. American Society of Civil Engineers (ASCE).

Cagua, B.; Aguiar, R.; Pilatasig, J. (2021). New Functions of CEINCI-LAB for the analysis and design of steel frame according to NEC-15. Revista Internacional de Ingeniería de Estructuras, 26(1),1-60.

Cagua, B.; Aguiar, R.; Pilatasig, J. (2021). New Functions of CEINCI-LAB for the analysis and design of steel frame with concentric bracing. Revista Internacional de Ingeniería de Estructuras, 26(2), 199-284.

Crisafulli, F. (2014). Diseño sismoresistente de estructuras de acero. Mendoza: Asociación Latinoamericana del Acero - Alacero.

Georgiev, T.; Raycheva, L. (2017). Influence of splitting beam and columns stiffnes ductile behaviour. Eurosteel. Copenhagen, Denmark.

Instituto Geofísico: Escuela Politécnica Nacional. (2016). Terremoto del 16 de abril de 2016. Quito: IGEPN.

Lara, M.; Aguirre, H.; Gallegos, M. (2018). Estructuras Aporticadas de Hormigón Armado que Colapsaron en el Terremoto del 16 de abril de 2016 en Tabunga-Ecuador. Revista Politécnica, 42(1).

Márquez, E.; Lobo-Q, W.; Vielma, J. (2015). Comportamiento de edificios de acero con diagonales concéntricas y excéntricas. Valparaíso: Pontificia Universidad Católica de Valparaíso.

NEC–SE–AC, Norma Ecuatoriana de la Construcción. (2015). Estructuras de Acero. Dirección de Comunicación Social MIDUVI.

NEC-SE-CG, Norma Ecuatoriana de la Construcción. (2015). Cargas (No Sísmicas). Dirección de Comunicación Social MIDUVI.

NEC-SE-DS, Norma Ecuatoriana de la Construcción. (2015). Peligro Sísimico-Diseño Sismo Resistente. Dirección de Comunicación Social MIDUVI.

Silva, A.; Castro, JM.; Monteiro, R. (2019). Practical considerations on the design of concentrically braced steel frames to Eurocode 8. Journal of constructional Steel Research, 158, 71-85.